1R.4 RADAR-LIDAR SYNERGY FOR SPACE-BASED RETRIEVAL OF WATER CLOUD PARAMETERS

Gregory May Herman Russchenberg*
Oleg Krasnov
Delft University of Technology, IRCTR, Delft, The Netherlands

Abstract

Knowledge of water clouds is essential for climate studies. To understand present global climate and predict climate changes, global observations of cloud microphysical properties are needed and space-based systems must be considered. Retrieval of cloud parameters from space challenges current technological possibilities; not just due to sensor limitations, but also due to complex relationships between cloud parameters and remote sensing observables. Straightforward retrieval of cloud microphysics with radar only, is hindered by the presence of drizzle. To overcome this problem, synergetic use of multiple sensors is employed. This paper focusses on the retrieval of the cloud liquid water content by means of spaceborne radar and lidar measurements. The combination of radar reflectivity and lidar optical extinction is used to classify clouds according to their drizzle fraction. Appropriate retrieval algorithms can then be applied to each category to obtain the liquid water content. As the method was initially developed for ground-based instruments, differences between sensing clouds from above and below were studied. Airborne data was then used to simulate space-based measurements and suitability of the technique for space-based applications was established. It is shown that accurate liquid water content retrieval from space is possible.

1 INTRODUCTION

It is generally assumed that changes in cloud radiative properties directly effect climate change (1), but knowledge of cloud microphysical properties is still insufficient for any quantitative analysis of these processes. To better understand the role of clouds on the atmosphere's radiative processes, further study of cloud microphysics is essential. To understand present global climate and detect and predict climate changes, global observations are needed and space based remote sensing must be considered.

One of the cloud properties that plays an important role in climate models, is the liquid water content (LWC). This paper focusses on the retrieval of the LWC of water clouds. A promising technique that makes use of ground based, collocated radar and lidar measurements to obtain the LWC in water clouds is described in (2) and (3). This technique makes use of the ratio of the radar reflectivity and the lidar optical extinction (Z/α) to classify a cloud into one of three types. Once the cloud type is known, the LWC can be derived from the radar reflectivity according to a cloud type specific $Z - LWC$ relationship.

In the near future several satellite missions that will study the impact of clouds on the earth's climate, are planned for launch. The CloudSat radar and the CALIPSO lidar systems of the National Aeronautics and Space Administration (NASA) will be launched in 2005. Furthermore, the European Space Agency is currently developing their EarthCARE mission, which is to address the interaction and impact of clouds and aerosols on the earth's radiative budget. In light of these developments, this paper studies the possibility of using space-based radar and lidar measurements to retrieve the LWC of water clouds.

The LWC retrieval method described in this paper was originally based on a ground-based radar and lidar system, sensing the clouds from below. In a space-based system, however, the radar and lidar would be sensing the clouds from above. To study whether this difference in viewpoint affects the retrieval method, ground-based data are compared to airborne measurements. Subsequently, airborne radar and lidar data were used to simulate space-based radar and lidar measurements. The LWC retrieval technique was then applied to both the airborne and the simulated spaceborne measurements and the results were compared. Validation took place by means of ground-based radiometer data.

* *Corresponding author address:* H.W.J. Russchenberg, Delft University of Technology, IRCTR, Delft, The Netherlands. E-mail: H.W.J.Russchenberg@irctr.tudelft.nl

The LWC retrieval technique and some implementation issues are discussed in sections 2 and 3. Section 4 describes the data set used for cloud parameter calculations and LWC retrieval. The results of this study are presented in section 5. Discussion of the results takes place in section 6 and the conclusions are presented in section 7.

2 THE LWC RETRIEVAL TECHNIQUE

The microphysical properties of water clouds can be parameterized in terms of liquid water content. Since both the liquid water content and the radar reflectivity are functions of the cloud particle size spectrum, the LWC can be derived from Z. Retrieval of LWC based on radar measurements alone is complicated by the presence of so-called drizzle droplets. A small number of these large drops can produce extremely large radar reflectivities, without contributing much to the LWC (4). Since the presence of drizzle in water clouds is more usual than its absence (5), application of a straightforward $Z - LWC$ relationship to the radar reflectivity to obtain the liquid water content, is hardly ever possible. A study by Krasnov and Russchenberg (2) shows that the combination of radar reflectivity and lidar optical extinction (i.e. the Z/α ratio) can be used to classify a cloud according to its drizzle fraction. The drizzle fraction then determines which $Z-LWC$ relationship is to be used for LWC retrieval. As the study presented in this paper makes use of the same method, the theoretical basis of this approach is described in this section.

To determine the $Z-LWC$ relationship and the relationship between the Z/α ratio and the drizzle fraction, in-situ cloud measurements from different field campaigns were used. For more information on the DYCOMS-II, CAMEX-3, CLARE'98 and BBC-I campaign, see (6), (7), (8) and (9) respectively.

2.1 *Cloud parameters from in-situ data*

The particle size spectrum of a cloud, as measured by in-situ probes, can be used to calculate various cloud parameters. Since dealing with water clouds, it is assumed that the spherical droplets act as Rayleigh scatterers for radar observations and as optical scatterers for lidar observations. Cloud parameters can then be computed from the drop size distribution using the following equations:

Radar reflectivity:

$$Z = 64 \cdot \sum_i N_i \cdot r_i^6 \cdot \Delta r_i, \qquad [mm^6 \cdot m^{-3}] \quad (1)$$

Lidar optical extinction:

$$\alpha = 2\pi \cdot \sum_i N_i \cdot r_i^2 \cdot \Delta r_i \cdot 10^{-6}, \qquad [m^{-1}] \quad (2)$$

Liquid water content:

$$LWC = \frac{4\pi\rho_w}{3} \cdot \sum_i N_i \cdot r_i^3 \cdot \Delta r_i \cdot 10^{-6}, \quad [g \cdot m^{-3}] \quad (3)$$

Effective radius:

$$R_{eff} = \frac{\sum_i N_i \cdot r_i^3 \cdot \Delta r_i}{\sum_i N_i \cdot r_i^2 \cdot \Delta r_i} \cdot 10^3, \qquad [\mu m] \quad (4)$$

where ρ_w [$kg \cdot m^{-3}$] is the density of water, N_i [$m^{-3} \cdot mm^{-1}$] is the number of particles (normalized by bin width) measured in the i^{th} bin, r_i [mm] is the droplet mid-radius and Δr_i [mm] is the width of the i^{th} bin. Unless stated otherwise, the measurement results of the cloud parameters presented in this paper are in the units as mentioned above.

2.2 *Cloud classification*

When combining radar and lidar for LWC retrieval, the amount of drizzle must be determined before application of the correct $Z - LWC$ relationship is possible. Since the Z/α ratio is proportional to the amount of drizzle, it can be used to classify a water cloud into one of three types (2):

The cloud without drizzle:

$$\log_{10}(Z/\alpha) \quad \leq -1 \quad (5)$$

The cloud with light drizzle:

$$-1 < \quad \log_{10}(Z/\alpha) \quad \leq 1.8 \quad (6)$$

The cloud with heavy drizzle:

$$\log_{10}(Z/\alpha) \quad > 1.8. \quad (7)$$

The threshold values were determined from the $(Z/\alpha) - R_{eff}$ relationship, as calculated from the drop size distributions of various measurement campaigns. Figure 1 clearly shows that the $(Z/\alpha) - R_{eff}$ relationship changes around $\log_{10}(Z/\alpha) = -1$ and around $\log_{10}(Z/\alpha) = 1.8$. The first change occurs at the

point where the influence of drizzle becomes visible. The second point of change can be used to mark the transition from light drizzle to heavy drizzle (2). Since the values in the figure are fairly scattered across the $(Z/\alpha) - R_{eff}$ plane, the threshold values may vary a bit. However, because the thresholds are only used for cloud classification and not for the actual LWC retrieval, the influence of this variability is limited.

This is illustrated using fig. 2, which depicts the $Z - LWC$ plane. The figure shows that different $Z - LWC$ relationships can be applied to the cloud data from the different classes. The solid lines represent the $Z - LWC$ relationships for the different classes. In the transitional area's, where one class crosses over into another, the relationships usually lie close together. This illustrates the limited influence of the Z/α threshold variability on the LWC retrieval. The different $Z - LWC$ relationships in different parts of the plane are presented in the next subsection.

2.3 *The Z - LWC relationships*

The solid lines in figure 2 represent the following $Z - LWC$ relationships:

For the cloud without drizzle (10) (11) (4):

$$Z = 0.048 \cdot LWC^{\,2.0} \quad (8)$$

$$Z = 0.03 \cdot LWC^{\,1.31} \quad (9)$$

$$Z = 0.012 \cdot LWC^{\,1.16} \quad (10)$$

For the cloud with light drizzle (12):

$$Z = 57.54 \cdot LWC^{\,5.17} \quad (11)$$

For the cloud with heavy drizzle (2):

$$Z = 323.59 \cdot LWC^{\,1.58} \quad (12)$$

The approximations of the $Z - LWC$ relationship for the cloud without drizzle are based on a theoretical model (eq. 8) or in-situ data from measurement campaigns other than the ones in the figure (equations 9 and 10). The approximation for the cloud with light drizzle was based on in-situ data from the CLARE'98 campaign and to determine the $Z - LWC$ relationship for the cloud with heavy drizzle CAMEX-3 and CLARE'98 data were used.

2.4 *LWC retrieval*

We have shown that, although the $Z - LWC$ plane is quite scattered and no single approximation is suitable for LWC retrieval from Z, once the cloud class is determined from the Z/α ratio, it is possible to retrieve the LWC by applying a different $Z - LWC$ approximation to each class. For the cloud without drizzle, equation 10 is used.

Because the lidar signal attenuates faster than the radar signal, only radar data will be available for some cloud area's. For area's where only radar data is available, classification is based on the following threshold values:

The cloud without drizzle:

$$\mathrm{dB}Z \leq -20 \quad (13)$$

The cloud with light drizzle:

$$-20 < \mathrm{dB}Z \leq -10 \quad (14)$$

The cloud with heavy drizzle:

$$\mathrm{dB}Z > -10 \quad (15)$$

The threshold values are chosen in such a way, that most of the cloud without drizzle and with heavy drizzle is classified correctly. Most of the cloud with light drizzle that is classified incorrectly will then be in area's of the $Z - LWC$ plane where one class crosses over into another. As the applied $Z - LWC$ relationships in those area's lie close together, the margin of error for the LWC retrieval will be limited.

3 IMPLEMENTATION OF THE RETRIEVAL TECHNIQUE

3.1 *Lidar optical extinction estimation*

The quantity measured by lidar is the lidar backscatter coefficient. The radar to lidar ratio (Z/α) used for cloud classification contains the lidar optical extinction α. The lidar optical extinction is obtained by applying an inversion algorithm to the lidar backscatter profiles. The inversion algorithm (described in (13)) makes use of a single absolute extinction as a reference value to calculate the rest of the extinction profile. The reference value for each profile is taken at the greatest distance from the ground where backscatter is present.

A low noise level is crucial for a stable inversion algorithm. Therefore, before applying the algorithm, a threshold noise level of 0.01 $\mathrm{km}^{-1}\cdot\mathrm{sr}^{-1}$ was determined and all values below this threshold were removed from the backscatter profile. Furthermore, individual profiles were smoothed by removing values with

one or less adjacent non-zero value (i.e. a value in the profile is considered noise when no non-zero value is present directly above *and* below). At spaceborne lidar resolutions smoothing was unnecessary, as the profiles were already smoothed due to the lower resolution.

3.2 *The radar to lidar ratio*

Simultaneous radar and lidar data is used to classify a cloud by calculating the Z/α ratio. Because radar and lidar systems usually have different resolutions, the number of data-points in a given volume differs for both instruments. To be able to calculate the Z/α ratio, linear interpolation was applied to obtain an equal number of data-points.

The radar and lidar measurements used in this study are from collocated instruments. It may therefore be assumed that the instruments are always sensing the same cloud. For this reason, and also because the data-sets proved most suitable for this approach, the radar and lidar data were synchronized in time and not in space.

3.3 *Simulating space-borne resolutions*

For the CLARE'98 measurement campaign airborne remote sensing data was available. As the airplane flies above the clouds, the nadir looking lidar and radar collect data that can be used to simulate space based measurements. To approximate satellite mounted radar and lidar resolutions, linear interpolation was applied to the original radar and lidar data to obtain resolutions representative for space based measurements.

The intended time resolution of the space grid depends on the spaceborne along-track resolution and the aircraft velocity. The aircraft velocity is used to determine the time period over which airborne data has to be averaged to simulate spaceborne horizontal resolution. The time resolution of the common grid is calculated using the following equation:

$$T_{res} = \frac{\mathrm{Horiz}_{res}}{V_{ac}} \tag{16}$$

where T_{res} [s] is the intended time resolution of the space grid, Horiz_{res} [m] the along-track resolution of the space-based instrument to be approximated and V_{ac} [m/s] the velocity of the aircraft carrying the radar and lidar.

For the approximation of the horizontal resolution of the space-based instruments, only the along-track resolution is considered. The cross-track resolution remains the original (airborne instrument) value.

The simulated spatial resolutions of the space-based instruments are based on the system characteristics of the CloudSat radar and the CALIPSO lidar. Both satellite systems are part of the Earth System Science Pathfinder (ESSP) Project and are expected to be launched in 2005. The radar has a vertical resolution of 500 m and an along-track resolution of 3.5 km (14). The lidar has a vertical resolution of 30 m and an along-track resolution of 333 m (15). Except for the lidar vertical resolution, the CloudSat and CALIPSO resolutions are used for the simulated spaceborne measurements. Since the simulated spaceborne lidar has a higher vertical resolution (30 m) than the available airborne lidar data (60 m averaging interval), the vertical resolution for the spaceborne lidar is set to 60 m. Since the CloudSat minimum detectable radar reflectivity is -26 dBZ, all simulated spaceborne radar data below this value is removed.

3.4 *Re-distributing spaceborne radar energy*

At spaceborne radar and lidar resolutions, the radar resolution cells are larger than the lidar resolution cells. Since the lowest resolution usually determines the resolutions in the common grid, one is inclined to base the common grid on the radar height and time resolutions. The common space grid, however, is based on the radar height resolution and the lidar time resolution. Due to differences in horizontal resolution, gaps in the cloud cover, for example, might be recognized as such by lidar, but perceived as cloud by radar. Due to a low resolution, radar energy from the cloud is spread out, covering (part of) the gap in the cloud cover. It is therefore assumed that there is no cloud, when in a vertical profile only radar data (and no lidar data) are present. The presence of the radar data is attributed to the poor radar resolution, which spreads out the radar energy over multiple horizontal lidar resolution cells. The radar energy from a single horizontal radar resolution cell is then re-distributed over the area of the cell corresponding to the horizontal resolution cells where lidar data were present. The new radar reflectivity value for each area where lidar data are present, is calculated using the following equation:

$$Z_{new} = Z_{old} + \frac{N_{empty}}{N_{lidar}} \cdot Z_{old} \tag{17}$$

where Z_{new} [$mm^6 \cdot m^{-3}$] is the new radar reflectivity value for the area of the radar cell where lidar data are

present, Z_{old} [$mm^6 \cdot m^{-3}$] is the initial radar reflectivity value of the entire radar cell, N_{empty} is the number of area's (with the width of a lidar resolution cell) in the radar cell corresponding to an empty vertical lidar profile and N_{lidar} is the number of area's corresponding to a non-empty lidar profile. Re-distribution of the radar energy results in more accurate radar data, with higher radar reflectivity values.

3.5 *Liquid Water Path*

The liquid water path (LWP) is a measure of the total amount of liquid water in a column of air. The LWP is calculated from the retrieved LWC, using the following equation:

$$LWP = \sum_i LWC_i \cdot h, \quad [g \cdot m^{-2}] \qquad (18)$$

where h [m] is the height interval of the resolution cells and LWC_i [$g \cdot m^{-3}$] is the LWC in the i^{th} cell.

The LWP measured by a radiometer is used to validate the retrieval method by comparing it to the LWP calculated from the radar derived LWC. In order to make an accurate comparison, the LWP from the radiometer is linearly interpolated to obtain the same time resolution as the derived LWP.

4 THE DATA-SET USED

The 1998 Cloud Lidar and Radar Experiment (CLARE'98) took place in Chilbolton (United Kingdom), in October 1998. CLARE'98 was part of the European Space Agency (ESA)'s Earth Observation Preparatory Programme.

At the Chilbolton site, cloud radar reflectivity was measured with the 95 GHz radar MIRACLE of the German research centre GKSS. The available radar data have a 10 s and 82.5 m averaging interval. The lidar optical extinction was derived from the profiles of backscatter coefficients, as measured by the 905 nm Vaisala CT75K ceilometer of the Dutch weather service KNMI. The available lidar data have a 30 s and 30 m averaging interval.

The Fokker 27 ARAT aircraft, owned by the French IPSL institute, carried both a radar (KESTREL) and a lidar (LEANDRE 1) system for airborne remote sensing. The KESTREL is a 95 GHz radar of the University of Wyoming and LEANDRE 1 is a backscattering lidar, operating at 532 nm and 1064 nm wavelength. The available radar data have a 1 s and 50 m interval of averaging. The available lidar data have a 1 s and 60 m interval of averaging.

CLARE'98 also provided LWP estimations from radiometer measurements. LWP data from the 93 GHz radiometer belonging to the University of Bath was used. The radiometer was situated at Chilbolton.

For this study, a suitable sub-set of the CLARE'98 data was selected, considering aspects as cloud cover, precipitation, ice-content and availability of simultaneous observations of multiple instruments. All the CLARE'98 data presented in this paper came from measurements that took place during run 51 on October 7, 1998.

5 RESULTS

5.1 *Ground-based vs. airborne remote sensing measurements*

The data from the ground-based MIRACLE radar at Chilbolton were compared to those from the airborne KESTREL radar (fig. 3). Because of the difference between the wind velocity and the aircraft velocity, the cloud coverage of the two radars, in a given period of time, differs. That is, the cloud moves over the ground-based radar more slowly, than the airborne radar moves over the cloud. To compensate for this difference, the airborne data consist of measurements taken between one minute before and after passing over Chilbolton, whereas the ground-based data consist of measurements taken between ten minutes before and after this moment. The same applies to the lidar backscatter data (see fig. 4).

The comparison indicates that, where the radars sense the same cloud, the lidar measurements show some differences. Differences in lidar measurements occur as the ground-based and airborne instruments sense different parts of the cloud. The nadir looking airborne lidar mainly senses the cloud top, whereas the ground-based lidar only senses the bottom of the cloud.

As a result of the differences in viewpoint of the ground-based and airborne lidar, Z/α data will be available for different parts of the cloud. This means that, for ground-based measurements, combined radar-lidar data will only be available for the bottom of the cloud, whereas for airborne measurements, the cloud top will provide the Z/α data. Even though different area's of the cloud have to be classified based on radar reflectivity only, classification remains reasonably stable. The effect of the differences

in viewpoint on the LWC retrieval is therefore limited. The histograms of the retrieved LWC in fig. 5 support this. The LWC retrieved from the ground-based measurements is similar to the LWC retrieved from the airborne measurements.

5.2 *Airborne vs. space-based measurements*

Airborne radar and lidar data were used to approximate space-based radar and lidar measurements. The resulting space-based data had similar values as their airborne equivalent. To be able to calculate the spaceborne Z/α ratio however, linear interpolation had to be applied to the spaceborne lidar data to match the resolution of the spaceborne radar data. This resulted in much lower optical extinction values. As a result the spaceborne Z/α data have larger values than the airborne data. However, in both cases, most of the Z/α values are between -1 and 1.8 and can be classified as light drizzle. The heavy drizzle is precipitating and can mainly be found in the area for which only radar data is available for classification. This area is not classified based on the Z/α ratio.

The final cloud classification for airborne and spaceborne data show good agreement. After classification the LWC was retrieved. Histograms of the LWC retrieved from airborne and spaceborne data are shown in fig. 6.

The LWP as calculated from the retrieved LWC from spaceborne data and the LWP from the Bath radiometer at Chilbolton, are shown in fig. 7. The ARAT aircraft passed over Chilbolton at 13.72 hours. The figure shows that at that time, both LWP's agree nicely.

Figure 7 also shows that when cloud classification is based on radar data only, the LWC retrieval is less accurate. This results in an overestimation of the LWC values.

6 DISCUSSION

6.1 *Ground-based vs. airborne remote sensing measurements*

Subsection 5.1 showed that although for different viewpoints, different parts of the cloud have to be classified on radar data only, cloud classification was hardly influenced. For both viewpoints, the radar retrieved LWC agreed nicely.

It must be noted that the compared cloud did not yield much radar reflectivity above -10 dBZ. These relatively large reflectivity values can belong to both the light and heavy drizzle categories. When classification is based on radar data only, radar reflectivity values above -10 dBZ are classified as heavy drizzle. Their presence could influence LWC retrieval when they cause light drizzle to be mistakenly classified as heavy drizzle. In a drizzle cloud however, light drizzle usually formes in the cloud top and the precipitating heavy drizzle will be mostly at the bottom of the cloud. When sensing the cloud from above, the light drizzle at the cloud top will be classified based on both radar and lidar, while the heavy drizzle at the bottom will be classified by radar alone. The heavy drizzle with radar reflectivity values above -10 dBZ will then be correctly classified by radar only. LWC retrieval from above should therefore work just as well (if not better) as from below.

6.2 *Airborne vs. space-based measurements*

As was described in subsection 5.2, linear interpolating the lidar data to match the radar resolution resulted in lower optical extinction values and higher Z/α values.

The majority of the Z/α values, nevertheless remains within the same cloud class. It is unlikely that an increase in the Z/α ratio, as a result of lower spaceborne lidar values, will result in false classification very often. The Z/α ratio will hardly ever be used to classify heavy drizzle, as heavy drizzle is mainly found at the bottom of the cloud, where classification will usually be based on radar data alone. The majority of the light drizzle data will not be at the heavy drizzle border and the bulk will remain within the same cloud class. Although some light drizzle on the border of the heavy drizzle class might be falsely classified due to increased Z/α values, this will nonetheless have limited influence on LWC retrieval, as $Z - LWC$ relationships approach each other at class borders. As for the cloud without drizzle, part of this class will be overlooked by spaceborne radar completely, due to limited instrument sensitivity. The remaining part will consist of data on the border of the light drizzle class. Wrongful classification, due to an increase in the Z/α ratio, will therefore have limited effect on the LWC retrieval.

Comparison of the histograms of the airborne and spaceborne radar retrieved LWC showed good agreement (see fig 6). Furthermore, fig. 7 showed that the LWP as calculated from the spaceborne LWC was similar to the LWP from the radiometer. Keep in mind that, as the ARAT aircraft flew over the cloud at much greater speed than that of the wind blowing the cloud

over the radiometer, airborne radar and lidar sensed a much larger cloud area than the ground-based radiometer. During the time period as depicted in fig. 7, the radiometer was sensing a cloud area with much less drizzle than the instruments on the aircraft. At the time the aircraft passed over Chilbolton (13.72 hours), the same, non-precipitating cloud area was sensed. At this time, the radiometer and calculated spaceborne LWP agree nicely.

For the classification based on radar data only, part of the light drizzle cloud was falsely classified as non-drizzle. This lead to an overestimation of the LWC, as was shown in fig. 7. It can therefore be concluded that radar-lidar synergy improves LWC retrieval from space.

7 CONCLUSION

The suitability of the liquid water content retrieval technique for space-based applications was established. It was shown that differences in viewpoint between radar-lidar cloud measurements from above and below hardly influences cloud classification and LWC retrieval.

Airborne data was used to simulate space-based measurements and study the suitability of the liquid water content retrieval technique for space-based applications. Airborne and spaceborne cloud classification and LWC retrieval show good agreement. The retrieved LWC values were validated with a ground-based radiometer. This shows that accurate liquid water content retrieval from space is possible.

Furthermore, it was shown that the combination of spaceborne radar and lidar produces a synergetic effect.

References

[1] U. Cubasch, R.D. Cess, ”Processes and modelling,” in *Climate Change: The IPCC Scientific Assessment*, Intergovernmental Panel on Climate Change (IPCC), J.T. Houghton, G.J. Jenkins and J.J. Ephraums, Eds. Cambridge: Cambridge University Press, 1990, pp. 69-91.

[2] O.A. Krasnov and H.W.J. Russchenberg, ”An enhanced algorithm for the retrieval of liquid water cloud properties from simultaneous radar and lidar measurements. Part I: The basic analysis of in situ measured drop size spectra,” in *Proc. ERAD*, 2002, pp. 173-178.

[3] O.A. Krasnov and H.W.J. Russchenberg, ”An enhanced algorithm for the retrieval of liquid water cloud properties from simultaneous radar and lidar measurements. Part II: Validation using ground based radar, lidar, and microwave radiometer data,” in *Proc. ERAD*, 2002, pp. 179-183.

[4] N.I. Fox and A.J. Illingworth, ”The retrieval of stratocumulus cloud properties by ground-based cloud radar,” *Journal of Applied Meteorology*, vol. 36, no. 5, pp. 485-492, 1997.

[5] H. Gerber, ”Microphysics of Marine Stratocumulus Clouds with Two Drizzle Modes,” *Journal of Atmospheric Sciences*, vol. 53, no. 12, pp. 1649-1662, 1996.

[6] B. Stevens, D. Lenschow, G. Vali, et al., ”Dynamics and Chemistry of Marine Stratocumulus-DYCOMS-II,” *Bulletin of the American Meteorological Society*, vol. 84, no. 5, pp. 579593, 2003.

[7] Global Hydrology Resource Center (GHRC). (2002, May). 3rd Convection and Moisture Experiment [Online]. Available: http://ghrc.nsstc.nasa.gov/camex3/

[8] European Space Agency (ESA), ”Clare’98: Cloud Lidar & Radar Experiment,” ESTEC, Noordwijk, The Netherlands, International Workshop Proceedings ISSN 1022-6656, October 1999.

[9] Royal Dutch Weather Service (KNMI). (2002, September). CLIWA-NET Homepage [Online]. Available: http://www.knmi.nl/samenw/cliwa-net/index.html

[10] D. Atlas, ”The estimation of cloud content by radar,” *Journal of Meteorology*, vol. 11, pp. 309-317, 1954.

[11] H. Sauvageot and J. Omar, ”Radar reflectivity of cumulus clouds,” *Journal of Atmospheric and Oceanic Technology*, vol. 4, pp. 264-272, 1987.

[12] R.J.P. Baedi, J.J.M. de Wit, H.W.J. Russchenberg, J.S. Erkelens and J.P.V. Poiares Baptista, ”Estimating Effective Radius and Liquid Water Content from Radar and Lidar Based on the CLARE98 Data-Set,” *Physics and Chemistry of the Earth*, vol. 25, no. 10-12, pp. 1057-1062, 2000.

[13] J.D. Klett, "Stable analytical inversion solution for processing lidar returns," *Applied Optics*, vol. 20, pp. 211-220, 1981.

[14] Colorado State University, Department of Atmospheric Science. Cloudsat : Payload Intrumentation [Online]. Available: http://cloudsat.atmos.colostate.edu/CSMinstrument.php

[15] NASA, Langley Research Center. CALIPSO - Instrumentation [Online]. Available: http://www-calipso.larc.nasa.gov/instrument/

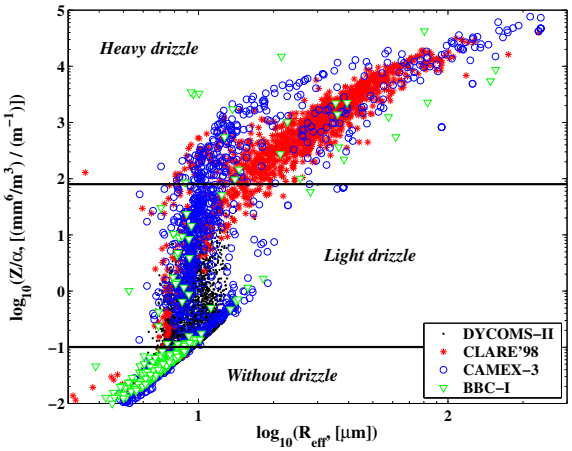

Figure 1: Radar to lidar ratio versus Effective radius for DYCOMS-II, CLARE'98, CAMEX-3 and BBC-I data

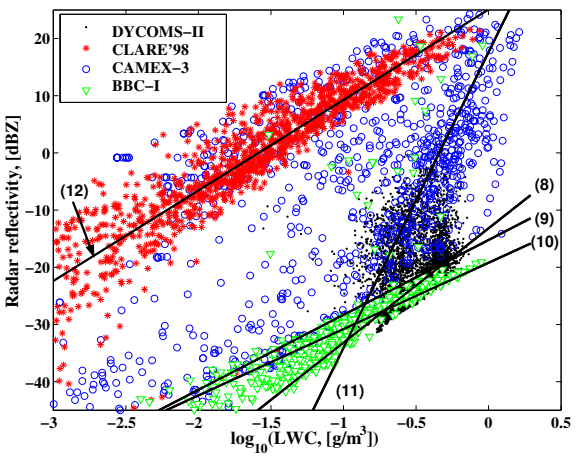

Figure 2: Radar reflectivity versus Liquid Water Content for DYCOMS-II, CLARE'98, CAMEX-3 and BBC-I data, including Z-LWC approximations with equation numbers

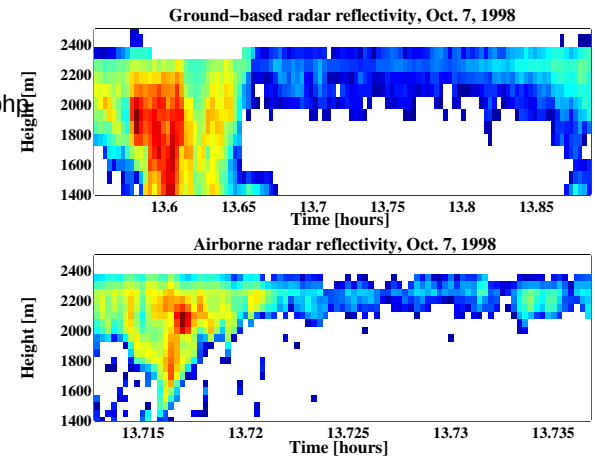

Figure 3: Ground-based MIRACLE and airborne KESTREL Radar reflectivity

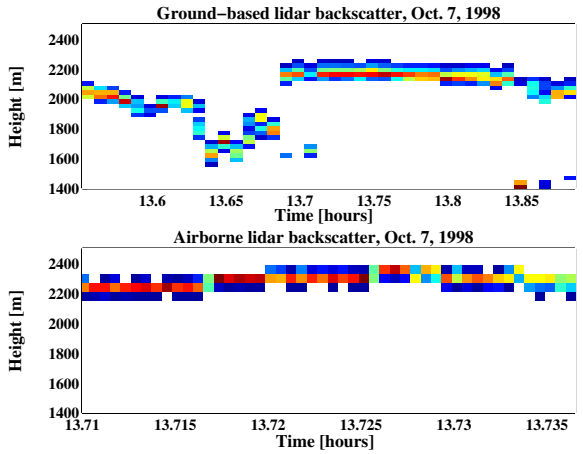

Figure 4: Ground-based Vaisala and airborne LEANDRE 1 Lidar backscatter

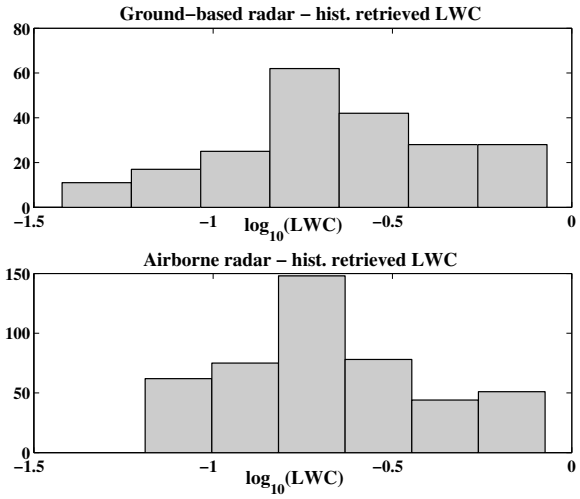

Figure 5: Histograms of the ground-based MIRACLE and airborne KESTREL radar retrieved LWC at Chilbolton, Oct. 7, 1998

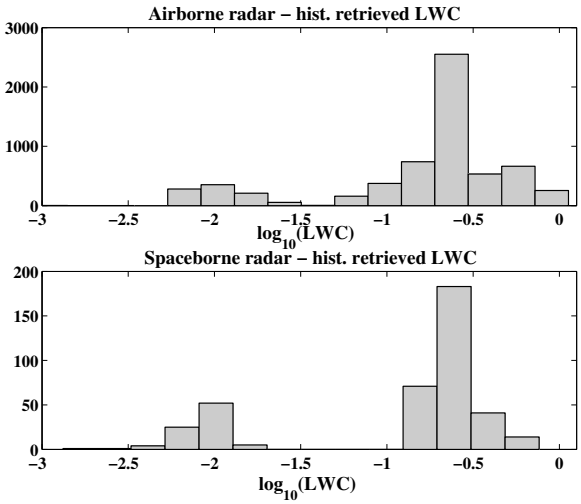

Figure 6: Histograms of the airborne and spaceborne radar retrieved LWC, Oct. 7, 1998

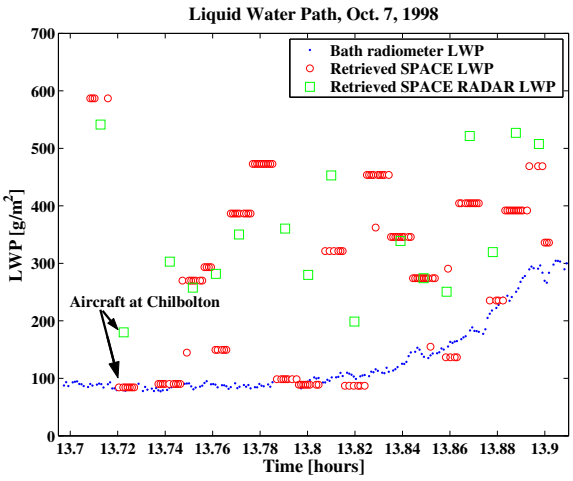

Figure 7: LWP from radiometer, spaceborne LWP with cloud class based on radar and lidar, and cloud class based on radar only